Optimal noisy quantum phase estimation with finite-dimensional states

Jin-Feng Qin[1,2,3] and Jing Liu[1,*]

[1]*Center for Theoretical Physics and School of Physics and Optoelectronic Engineering, Hainan University, Haikou 570228, China*

[2]*Mingde College, Chengdu Technological University, Yibin 644000, China*

[3]*School of Physics, Huazhong University of Science and Technology, Wuhan 430074, China*

(Received 10 August 2025; accepted 17 April 2026; published 5 May 2026)

Phase estimation in quantum interferometry is a major scenario where the quantum advantage is significantly revealed. Recently, the optimal finite-dimensional probe states (OFPSs) for phase estimation in two-mode quantum interferometry have been provided with the absence of noise [Qin *et al.*, Phys. Rev. A **112**, 052428 (2025)]. However, the noise is inevitable in practice and the previously obtained OFPSs may cease to be optimal anymore. Hence, the forms of the true OFPSs in the existence of various noises are still open questions. Here, the noise of particle loss is studied and the true OFPSs under this noise have been investigated with the numerical algorithm named constrained optimization by linear approximation. Furthermore, a two-step measurement strategy is proposed to realize the ultimate precision limit in practice. The validity of this strategy is confirmed by the numerical simulation of practical experiments.

DOI: 10.1103/l752-sl6p

I. INTRODUCTION

Phase estimation in quantum interferometry is the first scenario that proves that the standard quantum limit can be overcome [1–3], and with years of development, it has become one of the most important topics in quantum metrology. To provide an optimal scheme for phase estimation, searching for the optimal probe state is always the first thing to do, and has certainly been given extensive attention in many years [4–17]. The Fock basis, of which the elements are the eigenstates of the number operator, is a common representation of quantum states in many quantum systems, especially the bosonic systems. Many finite-dimensional states in the Fock basis are proved to be very powerful in quantum metrology [16,18–27], such as the well-known twin-Fock state [16,18–20] and N00N state [21–24]. However, the consistency between the average particle number and state dimension in these states makes it difficult to distinguish the contributions of the average particle number and state dimension to the final precision. Hence, investigations on those finite-dimensional states with inconsistent average particle number and state dimension become an emerging topic [28–36] in recent years, especially searching for the optimal ones in various scenarios [33–36].

Recently, Lee *et al.* [33] provided the optimal finite-dimensional probe state (OFPS) with respect to a fixed average particle number for the phase estimation in a single-mode bosonic system. Thereafter, the OFPSs for estimating the phase difference in both linear and nonlinear two-mode quantum interferometries have been given and thoroughly discussed [34] with the absence of noise. Moreover, it has been shown that both parity [37–41] and particle-counting (PC) [42–46] measurements are optimal measurements for the OFPS at the point of true value. The dependence of the optimality of these two measurements on the true value can be well eliminated via the adaptive measurements, where a tunable phase is involved and tuned based on the sharpness or other quantities [47–55]. The proposed scheme with the OFPS provides an aspect to enhance the measurement precision of phase difference without increasing the particle number of the probe. This scheme would be very useful in scenarios like biological detection [56], where a weak light probe is required to avoid damaging the biological specimen, and in cost-effective environments including the satellites [57] and chips [58]. It would also be very useful in the scenarios where the noise floor is strongly related to the particle number.

For the sake of providing a rigorous analytical result, the OFPS in the two-mode interferometry is first studied in the ideal scenario; namely, no noise is involved. However, the existence of noise is inevitable in practice. In quantum interferometry, the particle loss is one of the major noise modes and has been widely investigated in recent years [59–67]. In the case that the particle loss exists, the found forms of the OFPS may cease to be optimal anymore, at least in mathematics. Therefore, what the true OFPSs are under particle loss and how they perform in practice are still open questions. Providing answers to these questions is the major motivation of this work.

When the noise of particle loss exists, the analytical optimization of the probe state becomes extremely hard, if not fully impossible, since the state is mixed, and numerical optimization methodology has to be involved. In this paper, the constrained optimization by linear approximation (COBYLA)

*Contact author: jing.liu@hainanu.edu.cn

algorithm [68–70] is used as the numerical method to locate the noisy OFPS for different amounts of particle loss. In contrast with the noiseless scenario, the parity and particle-counting measurements are no longer optimal under particle loss, and in this case, the optimal measurement can be constructed via the eigenvectors of the symmetric logarithmic derivative. Unfortunately, this measurement is unrealizable in practice due to its dependence on the true value. To solve this problem, a two-step measurement strategy is proposed and its validity in practice is confirmed by numerical simulations of the experiments.

II. THEORETICAL MODEL AND DEPICTION OF THE PRECISION LIMIT

A common way to accumulate phase in a single-mode bosonic system is usually realized by the operator $\exp(i\phi_a a^\dagger a)$, with a the annihilation operator of the mode and ϕ_a the accumulated phase. In a two-mode bosonic system with a and b the annihilation operators, the total phase accumulation for both modes is $\exp(i\phi_a a^\dagger a + i\phi_b b^\dagger b)$, with ϕ_b the accumulated phase on mode b. Utilizing the Schwinger operator $J_z = (a^\dagger a - b^\dagger b)/2$ and number operator $n = a^\dagger a + b^\dagger b$, the total phase accumulation can be rewritten into

$$e^{i\phi_{\rm tot} n/2} e^{i\phi J_z} =: U_{\rm lin}, \tag{1}$$

where $\phi_{\rm tot} = \phi_a + \phi_b$ is the total phase and $\phi = \phi_a - \phi_b$ is the phase difference. This type of phase shift is usually called the linear phase shift since the accumulation operator $\phi_a a^\dagger a$ is proportional to $a^\dagger a$. When the accumulation operator is proportional to the kth power of $a^\dagger a$, i.e., $\phi_a (a^\dagger a)^k$, the corresponding phase shift is usually called the nonlinear phase shift. In this paper, we only consider the nonlinear case with $k = 2$, which can be readily realized in the current experiments. The nonlinear cases with higher powers will be further investigated in the near future. When both phase shifts on two modes are nonlinear with $k = 2$, the total phase accumulation is expressed by

$$e^{i\phi_{\rm tot}[(a^\dagger a)^2 + (b^\dagger b)^2]/2} e^{i\phi n J_z} =: U_{\rm non}. \tag{2}$$

Although two phases $\phi_{\rm tot}$ and ϕ exist in the operators $U_{\rm lin}$ and $U_{\rm non}$, their absolute values cannot be directly measured simultaneously without an external reference. In the meantime, if the absolute value of ϕ_a or ϕ_b is needed to be measured, the absolute value of the other one has to be known in principle, which means that the final precision of the unknown phase would be limited by the precision of the known phase. In this sense, the quantum advantage of the interferometry could be fully useless as long as the known phase is measured in a traditional way and its precision is limited by the standard quantum limit. Therefore, in this work we focus on the estimation of the phase difference ϕ that would avoid the aforementioned problems. Both linear and nonlinear phase shifts will be studied.

Particle loss is a common noise mode in quantum phase estimation, which in theory can be modeled by the fictitious beam splitter [59–61]. In a two-mode bosonic quantum interferometric model, the particle losses on two modes are usually modeled by two fictitious beam splitters. Recall that the modes a and b are those of both arms. The operators for the fictitious beam splitters can be written as

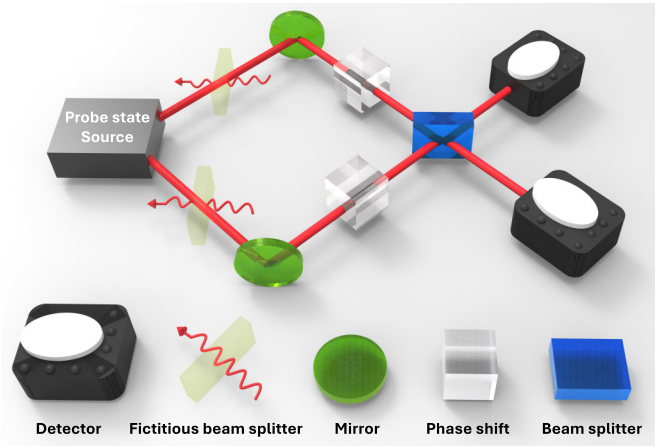

FIG. 1. Illustration of the phase estimation and particle loss in the scenario of the quantum optical interferometry. The light-green blocks represent the fictitious beam splitters, which are used to depict the particle loss in theory.

$$B_{ac}^{T_1} = e^{i\frac{\eta_1}{2}(a^\dagger c + a c^\dagger)}, \tag{3}$$

$$B_{bd}^{T_2} = e^{i\frac{\eta_2}{2}(b^\dagger d + b d^\dagger)}, \tag{4}$$

where c and d are two fictitious modes representing the particle loss. $T_1 = \cos^2(\eta_1/2)$ and $T_2 = \cos^2(\eta_2/2)$ are the transmission coefficients. In the case that T_1 (T_2) equals 1, no loss happens from the mode a (b), and when T_1 (T_2) equals zero, all particles are lost from the mode a (b). It has been shown that [59–61] the results would be the same when the particle loss occurs before or after the state goes through the phase shifts. Hence, here we take the case that the particle loss occurs first, and in this case the state going through the phase shifts is actually a mixed state. To better present the physical scenario we discuss, the phase estimation and particle loss are illustrated in Fig. 1 via the example of quantum optical interferometry. Notice that the light-green and blue blocks represent the fictitious and physical interferometer beam splitters, respectively. However, the main results of this work are not limited to this scenario.

The full quantum state of all modes a, b, c, and d before the particle loss happens can be written as $|\psi_{\rm in}\rangle \otimes |0\rangle_c \otimes |0\rangle_d$, where $|\psi_{\rm in}\rangle$ is the probe state on modes a and b. $|0\rangle_c$ ($|0\rangle_d$) is the vacuum state of the fictitious mode c (d), and $\otimes$ represents the tensor product. Based on the fictitious beam splitter operators given in Eqs. (3) and (4), the full state going through the fictitious beam splitters is

$$|\psi\rangle = B_{bd}^{T_2} B_{ac}^{T_1} |\psi_{\rm in}\rangle \otimes |0\rangle_c \otimes |0\rangle_d. \tag{5}$$

By tracing out the unobserved environmental modes c and d, the reduced density matrix on modes a and b is

$$\rho = {\rm Tr}_{cd}\left(B_{bd}^{T_2} B_{ac}^{T_1} |\psi\rangle\langle\psi| {B_{ac}^{T_1}}^\dagger {B_{bd}^{T_2}}^\dagger\right), \tag{6}$$

where ${\rm Tr}_{cd}(\cdot)$ is the partial trace on modes c and d. The parametrized state then reads $\rho_\phi = U_{\rm lin}\rho U_{\rm lin}^\dagger$ and $\rho_\phi = U_{\rm non}\rho U_{\rm non}^\dagger$ for the linear and nonlinear phase shifts, respectively.

In the quantum parameter estimation, the quantum Cramér-Rao bound (also known as Helstrom bound) is one of the most well-used tools to depict the precision limit. In this theory, the precision of the phase difference is depicted by the variance $\delta^2\phi$. Furthermore, the variance satisfies the following inequality [71,72]:

$$\delta^2\phi \geqslant \frac{1}{\mu I} \geqslant \frac{1}{\mu F}. \tag{7}$$

Here, μ is the repetition number of the experiment, and I and F are, respectively, the classical Fisher information (CFI) and quantum Fisher information (QFI). For a set of discrete probability distribution $\{p_i\}$, the CFI can be calculated via the equation $I = \sum_i (\partial_\phi p_i)^2/p_i$. Here, ∂_ϕ is short for $\partial/\partial\phi$. For the density matrix ρ_ϕ, the QFI can be calculated via the expression $F = \mathrm{Tr}(\rho_\phi L^2)$ [71,72]. Here, L is the symmetric logarithmic derivative (SLD) and is determined by the equation $\partial_\phi \rho_\phi = (\rho_\phi L + L\rho_\phi)/2$.

Now, denote the spectral decomposition of ρ in Eq. (6) as $\rho = \sum_{\lambda_i \in \mathcal{S}} \lambda_i |\lambda_i\rangle\langle\lambda_i|$, with λ_i and $|\lambda_i\rangle$ the ith eigenvalue and eigenstate of ρ and $\mathcal{S} = \{\lambda_i \in \{\lambda_i\} | \lambda_i \neq 0\}$. According to the expression of the QFI for unitary parametrization processes [73–75], the QFI for the linear phase shifts can be calculated by

$$F = \sum_{\lambda_i \in S} 4\lambda_i \mathrm{var}_{|\lambda_i\rangle}(J_z) - \sum_{\substack{\lambda_i,\lambda_j \in S \\ i\neq j}} \frac{8\lambda_i\lambda_j}{\lambda_i + \lambda_j} |\langle\lambda_i|J_z|\lambda_j\rangle|^2, \tag{8}$$

where $\mathrm{var}_{|\lambda_i\rangle}(J_z) := \langle\lambda_i|J_z^2|\lambda_i\rangle - \langle\lambda_i|J_z|\lambda_i\rangle^2$. For the nonlinear phase shifts, the expression of the QFI can be obtained by replacing J_z with nJ_z in the equation above. In this work, the QFI will be used as the objective function for the optimization.

III. THE NOISELESS OFPS

The finite-dimensional states are well studied in the quantum parameter estimation and constantly compared to the continuous-variable states, especially in the two-mode systems. In the past, the study of two-mode finite-dimensional states usually focused on the form $\sum_{i=0}^{N} c_i |i, N-i\rangle$, with $|i, N-i\rangle$ a Fock state and c_i a complex coefficient. The advantage of this form is that the average particle number is always fixed and can be readily realized in quantum systems like cold atoms in a double-well potential. However, the disadvantage is that the average particle number always equals to the dimension of the state minus one, and their contributions to the enhancement of the final precision cannot be distinguished. For the sake of investigating the effect of the state dimension on the precision, a more general form should be used, which reads

$$|\psi\rangle = \sum_{i,j=0}^{N} c_{ij} |ij\rangle. \tag{9}$$

Here, N is referred to as the Fock dimension and $|ij\rangle$ is a Fock state. c_{ij} is a complex coefficient. The average particle number (denoted by $\bar{n}$) for this state is

$$\bar{n} = \sum_{i,j=0}^{N} |c_{ij}|^2 (i+j), \tag{10}$$

which could be chosen as any value in the region $[0, 2N]$. Hence, the contributions of the average particle number and the Fock dimension can be identified independently.

Based on the form in Eq. (9), the OFPS can be analytically or numerically obtained by maximizing the QFI. Recently, the OFPSs for this case have been analytically provided in the absence of noise [34]. The form of the OFPS relies on the region of $\bar{n}$. For the linear phase shifts, in the region $\bar{n} \in (0, N]$ the OFPS reads

$$\sqrt{\frac{N-\bar{n}}{N}}|00\rangle + \sqrt{\frac{\bar{n}}{2N}}(e^{i\theta_1}|0N\rangle + e^{i\theta_2}|N0\rangle), \tag{11}$$

where $\theta_1, \theta_2 \in [0, 2\pi)$ are the relative phases. In the region $\bar{n} \in [N, 2N)$, the OFPS reads

$$\sqrt{\frac{2N-\bar{n}}{2N}}(e^{i\theta_1}|0N\rangle + e^{i\theta_2}|N0\rangle) + \sqrt{\frac{\bar{n}-N}{N}}|NN\rangle. \tag{12}$$

The QFIs for the states in Eqs. (11) and (12) are $\bar{n}N$ and $N(2N-\bar{n})$, respectively.

For the nonlinear phase shifts, in the region $\bar{n} \in (0, N]$, the OFPS is still the state given in Eq. (11). Furthermore, in the region $\bar{n} \in [N, \lfloor\frac{4N+1}{3}\rfloor]$, the OFPS is

$$\begin{aligned}&\sqrt{\frac{\bar{n}-\lfloor\bar{n}\rfloor}{2}}(|\lfloor\bar{n}\rfloor + 1 - N, N\rangle + e^{i\theta_1}|N, \lfloor\bar{n}\rfloor + 1 - N\rangle) \\ &+ \sqrt{\frac{1-(\bar{n}-\lfloor\bar{n}\rfloor)}{2}}(e^{i\theta_2}|\lfloor\bar{n}\rfloor - N, N\rangle + e^{i\theta_3}|N, \lfloor\bar{n}\rfloor - N\rangle),\end{aligned} \tag{13}$$

where θ_1, θ_2, and θ_3 are the relative phases. The symbol $\lfloor\cdot\rfloor$ represents the floor function. In this case, if $\bar{n}$ is an integer, the state above reduces to

$$\frac{1}{\sqrt{2}}(|\bar{n}-N, N\rangle + e^{i\theta}|N, \bar{n}-N\rangle), \tag{14}$$

with θ a relative phase. Furthermore, in the region $\bar{n} \in [\lfloor\frac{4N+1}{3}\rfloor, 2N)$, the OFPS is

$$\sqrt{\frac{2N-\bar{n}}{2(N-\zeta)}}(e^{i\theta_1}|\zeta N\rangle + e^{i\theta_2}|N\zeta\rangle) + \sqrt{\frac{\bar{n}-N-\zeta}{N-\zeta}}|NN\rangle. \tag{15}$$

Here, $\zeta = \lfloor\frac{N+1}{3}\rfloor$, and θ_1, θ_2 are the relative phases. If $N/3$ is an integer, the OFPS in this case reduces to

$$\sqrt{\frac{3(2N-\bar{n})}{4N}}\left(e^{i\theta_1}\left|\frac{N}{3}, N\right\rangle + e^{i\theta_2}\left|N, \frac{N}{3}\right\rangle\right) + \sqrt{\frac{3\bar{n}-4N}{2N}}|NN\rangle. \tag{16}$$

These OFPSs are analytically obtained in the ideal case, namely, without considering the existence of any noise. Their performance under the noise of particle loss has been thoroughly studied and compared to other finite-dimensional states like the N00N state and twin-Fock state in Ref. [34]. When the noise of particle loss exists, the aforementioned OFPSs may no longer be optimal anymore in mathematics. In the optimization process, the diagonalization of ρ_ϕ is usually required, which makes it difficult to search the OFPS analytically in this case. Hence, numerical methods are the first choice in this work to locate the true OFPS under particle loss.

IV. TRUE OFPS UNDER PARTICLE LOSS

In finite-dimensional probe state optimization, the constraint of a fixed input average particle number $\bar{n}$ makes it a constrained optimization problem. For the finite-dimensional state given in Eq. (9), the constrained optimization problem can be formulated as

$$\max_{C_{ij}} F(C_{ij})$$
$$\text{s.t.} \begin{cases} |C_{ij}| \in [0,1], \quad \forall i,j \in [0,N], \\ \sum_{i,j=0}^{N} |C_{ij}|^2 = 1, \\ \sum_{i,j=0}^{N} |C_{ij}|^2 (i+j) = \bar{n}, \end{cases} \tag{17}$$

where the symbol "s.t." is short for "subject to." Hence, in this case an efficient constrained optimization algorithm is required. Fortunately, Powell [68–70] developed a very powerful algorithm, the COBYLA algorithm, which fits the problem in our case. For the sake of simplification of the problem, here we take C_{ij} as a real coefficient to reduce the number of the variables in the optimization.

The COBYLA algorithm is a gradient-free optimization method for constrained nonlinear optimization problems [68–70]. The core philosophy of this algorithm is the linear approximations of the objective and constraint functions at the vertices of the simplices via linear interpolation, and then solving the approximated linear optimization problem with simplex methods. This algorithm can be directly invoked with the function *minimize(method='COBYLA')* or *fmin_cobyla()* in the Python package SciPy. Moreover, this state optimization scenario will be integrated into the package QuanEstimation [76,77] soon.

Utilizing the COBYLA algorithm, the true OFPS under particle loss can be identified. As a demonstration, the located noisy OFPS for $T_1 = T_2 = 0.8$ in the case of $\bar{n} = 2$ and $N = 6$ is illustrated in Fig. 2(a), which shows that the noiseless OFPS indeed ceases to be optimal anymore. The numerical optimization finishes when the variety of the optimized QFI converges to the scaling of 10^{-6}. Furthermore, random phases are added to the optimized coefficients to test the validity of the real optimal coefficients. As shown in Fig. 2(b), 10 000 groups of random phases are generated and added to the real optimal coefficients. The corresponding QFIs for these states (blue dots) are no larger than the one with real optimal coefficients (red line). This fact indicates that the optimal solution indeed exists for real coefficients in this case. In fact, in a specific case one can combine these two steps to locate the noisy OFPS with complex coefficients.

It is not difficult to realize that the formula of the noisy OFPS relies on the values of the transmission coefficients. To investigate the behavior of the maximum precision limit with different transmission coefficients, 100 noisy OFPSs are obtained via the COBYLA algorithm in both linear and nonlinear cases with $N = 6$ and $\bar{n} = 2, 8$. The program was run on a cluster with each node having 56 CPUs (2.7 GHz) and 240 GB memory. The values of the QFI with respect to the noisy OFPSs in the regions of $\bar{n} < N$ ($\bar{n} = 2$) and $\bar{n} > N$ ($\bar{n} = 8$) are given in Figs. 3(a1) and 3(a2) for the linear phase shifts,

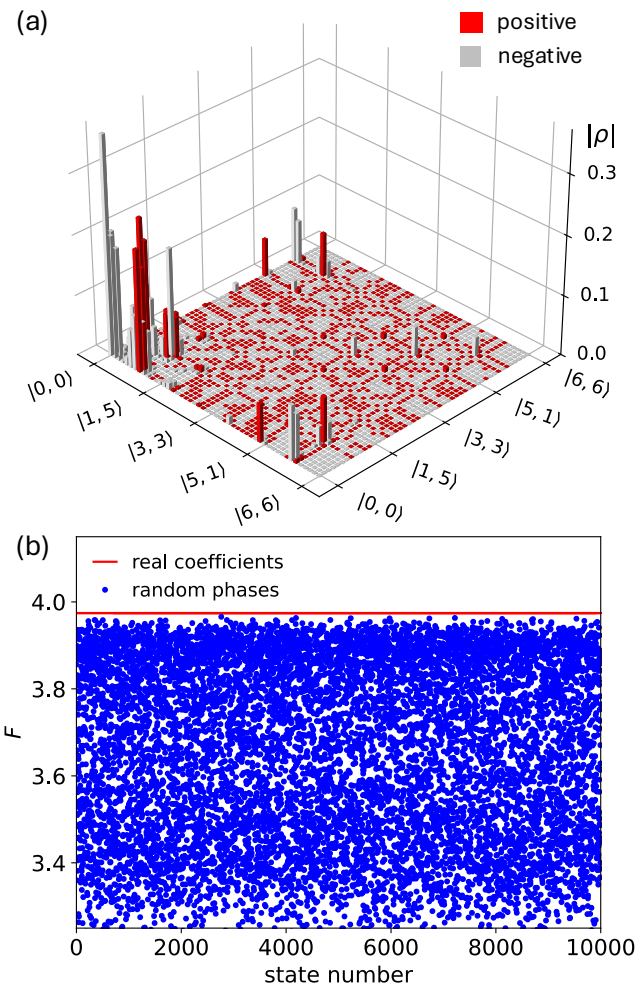

FIG. 2. (a) Tomography of the noisy OFPS obtained via COBYLA for $T_1 = T_2 = 0.8$ in the case of $\bar{n} = 2$ and $N = 6$. The red and gray bars represent that the value of the corresponding entry is positive and negative, respectively. (b) Validity test of the noisy OFPS obtained with real coefficients. Ten thousand groups of random phases (blue dots) are generated and used for the test. The red line represents the QFI for the noisy OFPS with real coefficients.

and Figs. 3(a3) and 3(a4) for the nonlinear phase shifts. The separation of the regions is due to the existence of different formulas of the noiseless OFPS in these two regions. In all figures, the negative effect of particle loss coincides with the general understanding that it becomes more significant when the values of T_1 and T_2 reduce. Since the formulas of the noisy OFPSs are usually more complex than their noiseless counterparts, the preparation of the noisy OFPSs might also be more complex in practice. Hence, a more important question here is when the noiseless OFPSs can still present comparable performance with the noisy OFPSs.

It is obvious that the comparable performance can only exist when the particle loss is not significant. Hence, the QFI for large transmission coefficients needs to be investigated for the sake of answering the aforementioned question. Denote $T_1 = 1 - \delta_1$ and $T_2 = 1 - \delta_2$ with δ_1 and δ_2 two small quantities, then the Taylor expansion of the ith eigenvalue

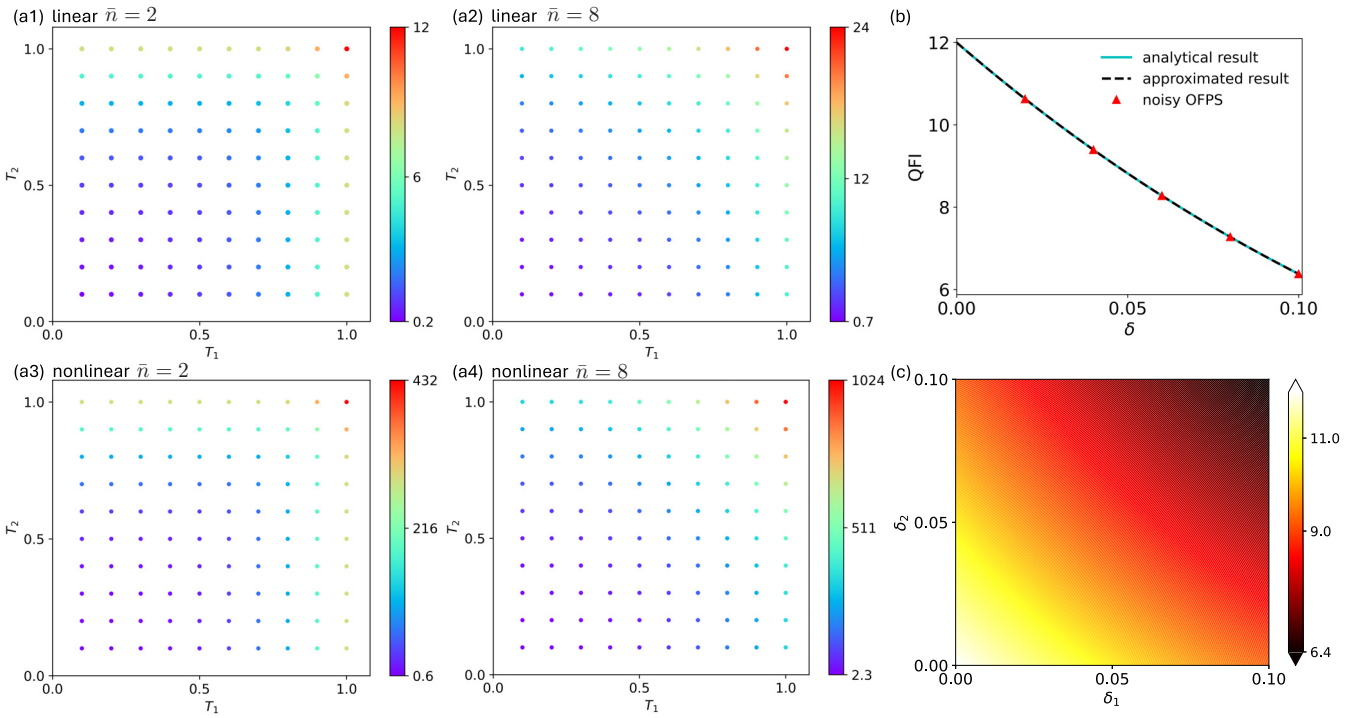

FIG. 3. The values of the QFI for the true OFPSs under particle loss as a function of transmission coefficients T_1 and T_2 for (a1) linear phase shifts with $\bar{n} = 2$ ($\bar{n} < N$); (a2) linear phase shifts with $\bar{n} = 8$ ($\bar{n} > N$); (a3) nonlinear phase shifts with $\bar{n} = 2$ ($\bar{n} < N$); and (a4) nonlinear phase shifts with $\bar{n} = 8$ ($\bar{n} > N$). (b) The values of QFI for the analytical (solid cyan line) and approximated (dashed black line) results regarding the noiseless OPFS and that of the noisy OFPSs (red triangles) for different values of δ ($\delta_1 = \delta_2 = \delta$). (c) The behaviors of the approximated QFI with respect to the noiseless OFPS given in Eq. (11) as a function of δ_1 and δ_2 in the linear case with $\bar{n} = 2$. $N = 6$ and ϕ_{true} is set to be 0.2 in all plots.

and eigenstate of ρ, up to the first order of δ_1 and δ_2, can be expressed by

$$\lambda_0 = 1 - \delta_1\lambda_{0,1} - \delta_2\lambda_{0,2}, \tag{18}$$

$$\lambda_i = \delta_1\lambda_{i,1} + \delta_2\lambda_{i,2}, \quad \forall i \neq 0 \tag{19}$$

and

$$|\lambda_0\rangle = |\psi_{\text{in}}\rangle + \delta_1|\lambda_{0,1}\rangle + \delta_2|\lambda_{0,2}\rangle, \tag{20}$$

$$|\lambda_i\rangle = \delta_1|\lambda_{i,1}\rangle + \delta_2|\lambda_{i,2}\rangle, \quad \forall i \neq 0. \tag{21}$$

Here, $\lambda_{0,1}$, $\lambda_{i,1}$ ($\lambda_{0,2}$, $\lambda_{i,2}$) and $|\lambda_{0,1}\rangle$, $|\lambda_{i,1}\rangle$ ($|\lambda_{0,2}\rangle$, $|\lambda_{i,2}\rangle$) are the first-order terms with respect to δ_1 (δ_2). The existence of λ_0 and $|\lambda_0\rangle$ is due to the fact that ρ is actually the pure state $|\psi_{\text{in}}\rangle$ when $T_1 = T_2 = 1$. Based on Eq. (8), the QFI with respect to ρ up to the first order (denoted by F_{lin}) in the linear case is

$$F_{\text{lin}} = 4\lambda_0\big(\langle\lambda_0|J_z^2|\lambda_0\rangle - \langle\lambda_0|J_z|\lambda_0\rangle^2\big). \tag{22}$$

Namely, the approximated QFI is just the QFI with respect to $|\lambda_0\rangle$ multiplying λ_0. When the probe state $|\psi_{\text{in}}\rangle$ is the noiseless OFPS given in Eq. (11) or (12), the term $\langle\psi_{\text{in}}|J_z|\psi_{\text{in}}\rangle$ vanishes, which means

$$F_{\text{lin}} \approx 4\lambda_0\big(\langle\lambda_0|J_z^2|\lambda_0\rangle\big). \tag{23}$$

This fact can be further confirmed by Fig. 3(b), where the behaviors of the analytical (solid cyan line) and approximated (dashed black line) results coincide with each other in the case of symmetric loss ($\delta_1 = \delta_2 = \delta$) with $\bar{n} = 2$ and $N = 6$. More importantly, the noiseless OFPS presents comparable performance with the noisy OFPSs (red triangles); hence, in this region of loss the noiseless OFPS would be a better choice as the probe state. Moreover, this result also indicates that in this region both the optimality and performance of the noiseless OFPS are very robust. As to the robustness of the noisy OFPSs in the entire region, it is difficult to define the robustness in this case since the form of the noisy OFPS relies on the loss rate. Different loss rates usually correspond to different noisy OFPSs. Therefore, further investigations are still needed to quantify the robustness against the loss in general.

Apart from the average particle number, the Fock dimension is another powerful resource in the OFPS to further improve the precision limit in the absence of noise [34]. However, the impact of loss on the effectiveness of the Fock dimension is still unknown. Due to the previous discussions, the noiseless OFPSs present comparable performance in the case that $T_1 = T_2 \geqslant 0.9$; hence, in this region the noiseless OFPSs can be used instead of the noisy OFPSs to reveal the influence of the particle loss on the effectiveness of the Fock dimension. As shown in Fig. 4, the QFIs of the noiseless OFPSs in the cases of $T_1 = T_2 = 0.98$ (purple diamonds) and 0.94 (green triangles) increase as the Fock dimension grows, indicating that Fock dimension is still an effective resource to improve the precision limit in this region. In the case that $T_1 = T_2 = 0.8$, the QFIs of the noiseless OFPSs (black squares) decrease as the Fock dimension grows. This fact means that if the noiseless OFPSs are still taken as the probe states in this case, Fock dimension ceases to be an effective resource. If the noisy

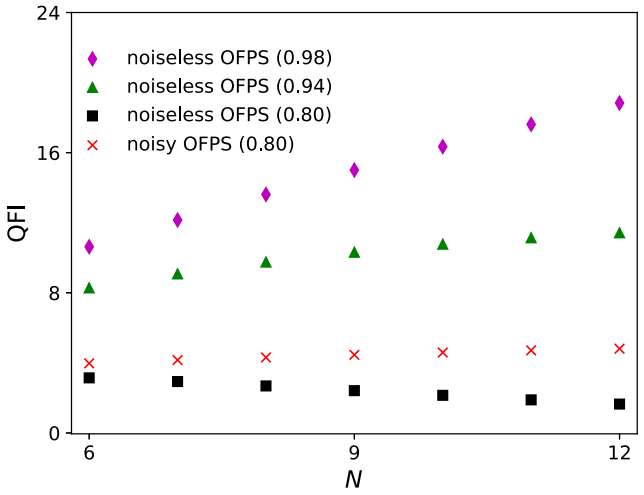

FIG. 4. The QFIs of the noiseless and noisy OFPSs with different values of the Fock dimension N. The purple diamonds, green triangles, and black squares represent the QFIs of the noiseless OFPSs for the transmission coefficients $T_1 = T_2 = 0.98, 0.94, 0.80$, respectively. The red crosses represent the QFIs of the noisy OFPSs with respect to $T_1 = T_2 = 0.8$. In the entire figure, $\bar{n} = 2$.

OFPSs are applied, the QFIs (red crosses) recover to a slowly growth trend. Hence, in this case the Fock dimension is still an effective resource when the noisy OFPSs are used. However, its efficiency on the performance improvement is limited.

V. OPTIMAL MEASUREMENT

A complete protocol for quantum phase estimation contains not only the probe state but also the measurement. To fit the usual form of the measurement in quantum interferometry, a beam splitter is added before the measurement is executed, as illustrated in Fig. 1. The theoretical operator for this beam splitter is $\exp(i\pi J_x/2)$, with $J_x = (a^\dagger b + ab^\dagger)/2$ a Schwinger operator.

With the absence of noise, both parity and particle-counting measurements are optimal to the OFPS for some specific true values [34]. The dependency of the optimality of these two measurements on the true value ϕ_{true} can be overcome by the adaptive measurement, where a tunable phase is involved and tuned properly. When the particle loss exists, both the parity and particle-counting measurements cease to be optimal with respect to the noisy OFPS, and even the noiseless OFPS. As a demonstration, the QFIs of the noisy OFPS (purple dots) and noiseless OFPS (black dots), and the CFI (green circle) of the PC measurement with respect to the noisy OFPS are illustrated in Fig. 5(a) in the case of $\bar{n} = 2$ and $N = 6$. The transmission coefficients are $T_1 = T_2 = 0.8$ and the true value ϕ_{true} is set to be 0.2. It can be seen that in

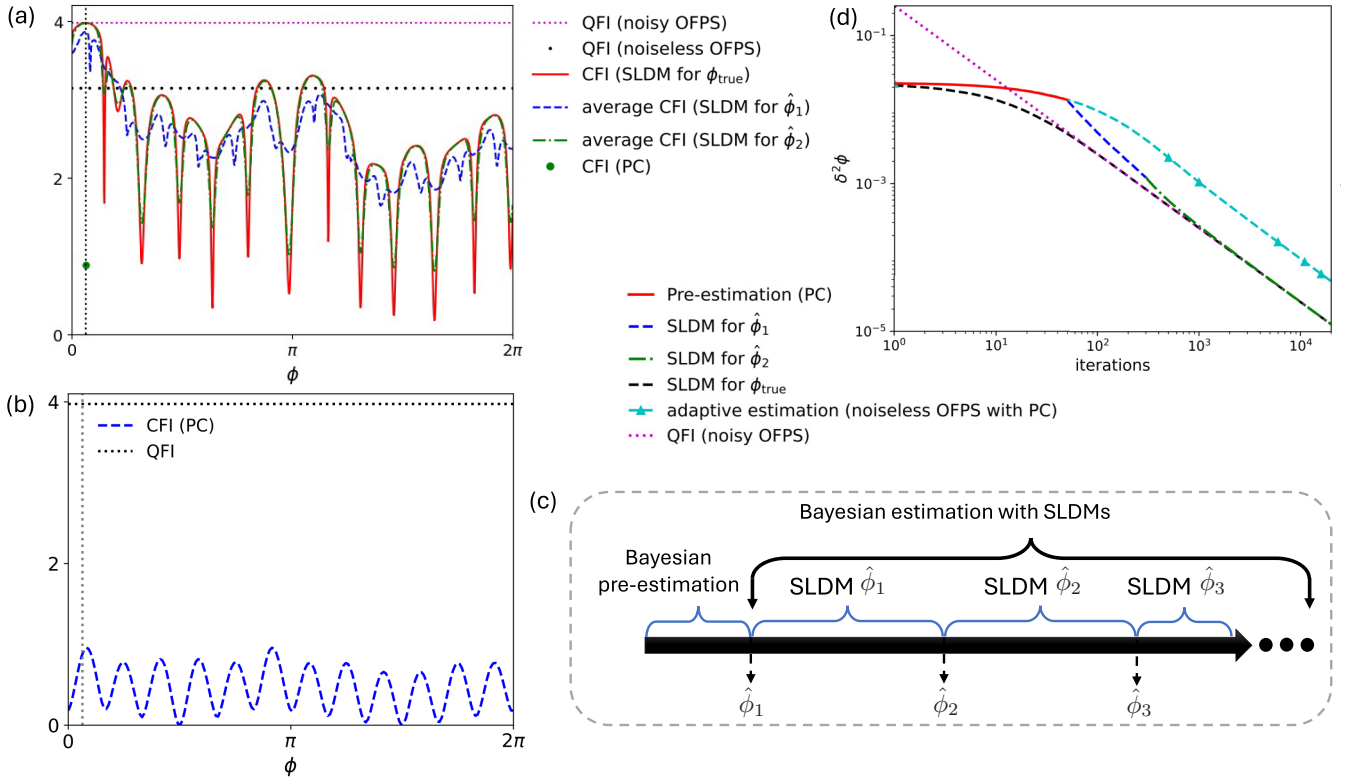

FIG. 5. (a) The behaviors of the QFI and CFI (or average CFI) for noisy and noiseless OFPSs as functions of phase difference ϕ. The average CFIs of the noisy OFPS correspond to the SLDM with different estimated values, and are the average of 2000 simulations. (b) The values of the CFI and QFI for the noisy OFPS with PC measurement in the entire region of ϕ. (c) Illustration of the two-step strategy to realize the optimal measurement without the knowledge of the true value. (d) Simulation of the performance of the two-step strategy in practice. All lines are the average performance of 2000 simulations. In panels (a), (b), and (d), the parameters are set as $\bar{n} = 2$, $N = 6$, and $T_1 = T_2 = 0.8$. The true value $\phi_{\text{true}} = 0.2$.

this case the noiseless OFPS indeed ceases to be optimal due to the large gap between its QFI and that of the noisy OFPS. In the meantime, the PC measurement is not an optimal measurement to the noisy OFPS. The CFI of the parity measurement is no larger than that of the PC measurement, and thus is not optimal either. Furthermore, although the performance of the adaptive PC measurement can reach the maximum CFI in the entire region of ϕ, it is still far from the value of the QFI, as shown in Fig. 5(b), which means that the performance of the adaptive measurement in this case is limited. Therefore, the optimal measurement of the noisy OFPS has to be located for the sake of providing a complete optimal scheme.

One simple way to construct the optimal measurement is using the eigenvectors of the SLD. Denote $|L_k\rangle$ as the kth eigenvector of L, then the projective measurement constructed via the SLD (SLDM) at the point of the true value (denoted by $\{e^{i\frac{\pi}{2}J_x}|L_k\rangle\langle L_k|e^{-i\frac{\pi}{2}J_x}\}_{\phi=\phi_{\text{true}}}$, the rotation of $e^{i\frac{\pi}{2}J_x}$ is used to cancel the effect of the second beam splitter) is the optimal measurement; i.e., the CFI of the SLDM at this point equals the QFI. Here, the CFI can be calculated via the equation

$$I=\sum_k \frac{(\partial_\phi\langle L_k|\rho_\phi|L_k\rangle)^2}{\langle L_k|\rho_\phi|L_k\rangle}. \tag{24}$$

The CFI of the SLDM in the case of $\bar{n}=2$ and $N=6$ is also illustrated in Fig. 5(a) (red line) as a demonstration. At the point of ϕ_{true}, as shown in the plot, the CFI of the SLDM reaches the QFI, indicating that it is indeed optimal at this value point.

Similar to the parity and PC measurements in the noiseless scenario, SLDM depends on the phase difference ϕ and is only optimal at the point $\phi=\phi_{\text{true}}$. However, in practice ϕ_{true} is not known, and more importantly, the choice of ϕ in the SLDM affects not only the optimality like the parity and PC measurements but also the specific form of the SLDM. Hence, when the particle loss exists we have to find a way to realize the optimal measurement without the knowledge of ϕ_{true}.

In this paper, we provide a two-step measurement strategy to realize the optimal measurement in practice without a high prior knowledge of the true value before the experiment, as illustrated in Fig. 5(c). The first step is the Bayesian pre-estimation. Both the parity and PC measurements can be used in this step. The PC measurement is usually more efficient and requires fewer iteration numbers. After the Bayesian pre-estimation, the estimated value $\hat{\phi}_1$ is obtained and used to construct the SLDM, i.e., $\{e^{i\frac{\pi}{2}J_x}|L_k\rangle\langle L_k|e^{-i\frac{\pi}{2}J_x}\}_{\phi=\hat{\phi}_1}$. The second step is the Bayesian estimation with the SLDM. In this step, several SLDMs are constructed with the estimated values of ϕ. For example, after proper iterations of the Bayesian estimation with $\{e^{i\frac{\pi}{2}J_x}|L_k\rangle\langle L_k|e^{-i\frac{\pi}{2}J_x}\}_{\phi=\hat{\phi}_1}$, an estimated value $\hat{\phi}_2$ is obtained and used to construct the second SLDM $\{e^{i\frac{\pi}{2}J_x}|L_k\rangle\langle L_k|e^{-i\frac{\pi}{2}J_x}\}_{\phi=\hat{\phi}_2}$, which is further applied in the estimation to obtain another estimated value. This process repeats until the precision converges. The iteration numbers of the pre-estimation and each SLDM need to be determined case by case in practice. Due to the limited performance of the Bayesian estimation with the parity or PC measurement under particle loss, the pre-estimation does not need too many iterations. The improvement would be very little once it converges.

The case of $\bar{n}=2$ and $N=6$ is still taken to demonstrate the performance of the given two-step strategy. The simulation of the experiment is given in Fig. 5(d). The PC measurement is chosen in the first step. The prior probability distribution of ϕ is a uniform one in the region $[0,\pi/6]$. After 50 iterations of pre-estimation (solid red line), $\hat{\phi}_1$ is obtained. In the second step, two SLDMs are constructed and applied. The first one is constructed via $\hat{\phi}_1$ and used in 250 iterations (dashed blue line). The second one is constructed via $\hat{\phi}_2$, which is obtained at the end of the 300th iteration, and used in the rest iterations (dash-dotted green line). All lines are the average of 2000 simulations. It shows that the result of the two-step strategy coincides with the theoretical optimal measurement $\{e^{i\frac{\pi}{2}J_x}|L_k\rangle\langle L_k|e^{-i\frac{\pi}{2}J_x}\}_{\phi=\phi_{\text{true}}}$ (dashed black line, also the average of 2000 simulations). And it reaches the precision limit given by the QFI (dotted purple line). This performance is way better than the adaptive PC measurement of the noiseless OFPS (solid-triangle cyan line, the average of 2000 simulations), and more technical details of the Bayesian and adaptive measurements can be found in Ref. [34]. To more intuitively understand the two-step strategy, the average CFIs of the SLDMs with respect to $\hat{\phi}_1$ and $\hat{\phi}_2$ are given in Fig. 5(a) as the dashed blue and dash-dotted green lines. It can be found that the values of the average CFI increase at the point of ϕ_{true} when the measurement changes from $\{e^{i\frac{\pi}{2}J_x}|L_k\rangle\langle L_k|e^{-i\frac{\pi}{2}J_x}\}_{\phi=\hat{\phi}_1}$ to $\{e^{i\frac{\pi}{2}J_x}|L_k\rangle\langle L_k|e^{-i\frac{\pi}{2}J_x}\}_{\phi=\hat{\phi}_2}$. More importantly, the performance of the SLDM $\{e^{i\frac{\pi}{2}J_x}|L_k\rangle\langle L_k|e^{-i\frac{\pi}{2}J_x}\}_{\phi=\hat{\phi}_2}$ basically coincides with the theoretical optimal measurement $\{e^{i\frac{\pi}{2}J_x}|L_k\rangle\langle L_k|e^{-i\frac{\pi}{2}J_x}\}_{\phi=\phi_{\text{true}}}$, especially at the point of ϕ_{true}. Hence, the given two-step strategy can indeed realize the optimal measurement of the noisy OFPS in practice and reach the ultimate precision limit.

VI. CONCLUSION

In conclusion, in this paper we have located the OFPSs for quantum phase estimation under the noise of particle loss. The performance of the noisy OFPSs is investigated for different amounts of particle loss. The noiseless OFPSs show a comparable performance with the noisy OFPSs in the case of small losses.

Optimal measurement is indispensable for a complete optimal phase estimation scheme. Different from the noiseless case, the parity and particle-counting measurements cease to be optimal under the noise of particle loss. The projective measurement constructed via the eigenvectors of the symmetric logarithmic derivative (SLDM) is then applied as the optimal measurement instead. To solve the problem of the dependence of the SLDM on the true value, which makes it unrealizable in practice, a two-step strategy based on the Bayesian estimation is proposed. Utilizing the numerical simulation of the practical experiment, this strategy is proved to be an efficient way to realize the ultimate precision limit quantified by the quantum Fisher information.

Quantum interferometry with the OFPSs provides a full approach, i.e., Fock dimension, to further improve the phase sensitivity without increasing the particle number of the probe. To make the OFPSs applicable in practice, their

preparations in various physical platforms are crucial and require deep investigations. Given the current quantum information techniques, quantum circuits appear to be the most promising platform for the practical implementation of OFPSs in the near future and worth further investigation. Moreover, the forms of the OFPSs for quantum multiphase estimation are still open questions and also worth to be further studied.

Particle loss is a common noise mode in quantum interferometry, yet not the only one. The preparation inefficiency of the probe state and the detector inefficiency are also very important noise sources [19,78,79]. The effect of the preparation inefficiency is similar to the particle loss, which also makes the state mixed before it goes into the phase shifts. Hence, the OFPSs under this noise can also be readily solved via the COBYLA algorithm. The involvement of detector inefficiency would be more completed. The form of the OFPS is not affected by the detector inefficiency in principle since the used objective function is the QFI. However, it is highly possible that the detector inefficiency would make it hard or even impossible to find the optimal measurement to attain the QFI of the OFPS. An alternative approach is to optimize the probe state and measurement simultaneously with the CFI as the objective function. The performance of this optimization process is hard to predict due to the general difficulty of multivariable optimizations. Therefore, the optimal phase estimation schemes with finite-dimensional states involving the detector inefficiency are still an open problem and need to be further investigated in the future. In the meantime, locating the noisy OFPSs poses a significant computational challenge for the COBYLA algorithm when the Fock dimension is large. State-of-the-art learning algorithms might be potential candidates to solve this problem.

Due to the importance of quantum interferometry in quantum information and technology, the proposed phase estimation scheme with the OFPSs would be very useful in practice. It has great potential to be applied soon in both quantum industry and fundamental research like gravitational-wave detections and tests of fundamental physics.

ACKNOWLEDGMENTS

This work was supported by the National Natural Science Foundation of China (Grants No. 12575013, No. 12547103, and No. 12175075).

DATA AVAILABILITY

The data that support the findings of this article are openly available [80].

[1] C. M. Caves, Quantum-mechanical radiation-pressure fluctuations in an interferometer, Phys. Rev. Lett. **45**, 75 (1980).
[2] C. M. Caves, Quantum-mechanical noise in an interferometer, Phys. Rev. D **23**, 1693 (1981).
[3] M. Xiao, L.-A. Wu, and H. J. Kimble, Precision measurement beyond the shot-noise limit, Phys. Rev. Lett. **59**, 278 (1987).
[4] B. Yurke, S. L. McCall, and J. R. Klauder, SU(2) and SU(1, 1) interferometers, Phys. Rev. A **33**, 4033 (1986).
[5] J. J. Bollinger, W. M. Itano, D. J. Wineland, and D. J. Heinzen, Optimal frequency measurements with maximally correlated states, Phys. Rev. A **54**, R4649(R) (1996).
[6] V. Giovannetti, S. Lloyd, and L. Maccone, and Quantum Metrology, Quantum metrology, Phys. Rev. Lett. **96**, 010401 (2006).
[7] L. Pezzé and A. Smerzi, Entanglement, nonlinear dynamics, and the Heisenberg limit, Phys. Rev. Lett. **102**, 100401 (2009).
[8] M. G. Genoni, S. Olivares, and M. G. A. Paris, Optical phase estimation in the presence of phase diffusion, Phys. Rev. Lett. **106**, 153603 (2011).
[9] R. Demkowicz-Dobrzański, Optimal phase estimation with arbitrary *a priori* knowledge, Phys. Rev. A **83**, 061802(R) (2011).
[10] P. C. Humphreys, M. Barbieri, A. Datta, and I. A. Walmsley, Quantum enhanced multiple phase estimation, Phys. Rev. Lett. **111**, 070403 (2013).
[11] M. Jarzyna and R. Demkowicz-Dobrzański, Matrix product states for quantum metrology, Phys. Rev. Lett. **110**, 240405 (2013).
[12] M. D. Lang and C. M. Caves, Optimal quantum-enhanced interferometry using a laser power source, Phys. Rev. Lett. **111**, 173601 (2013).
[13] J. Sahota and N. Quesada, Quantum correlations in optical metrology: Heisenberg-limited phase estimation without mode entanglement, Phys. Rev. A **91**, 013808 (2015).
[14] S. Altenburg, S. Wölk, G. Tóth, and O. Gühne, Optimized parameter estimation in the presence of collective phase noise, Phys. Rev. A **94**, 052306 (2016).
[15] S. Ragy, M. Jarzyna, and R. Demkowicz-Dobrzański, Compatibility in multiparameter quantum metrology, Phys. Rev. A **94**, 052108 (2016).
[16] M. D. Lang and C. M. Caves, Optimal quantum-enhanced interferometry, Phys. Rev. A **90**, 025802 (2014).
[17] S. Mondal, P. Ghosh, and U. Sen, Optimal quantum precision in noise estimation: Necessity of entanglement, Phys. Rev. A **113**, 042449 (2026).
[18] M. J. Holland and K. Burnett, Interferometric detection of optical phase shifts at the Heisenberg limit, Phys. Rev. Lett. **71**, 1355 (1993).
[19] A. Datta, L. Zhang, N. Thomas-Peter, U. Dorner, B. J. Smith, and I. A. Walmsley, Quantum metrology with imperfect states and detectors, Phys. Rev. A **83**, 063836 (2011).
[20] X.-Y. Luo, Y.-Q. Zou, L.-N. Wu, Q. Liu, M.-F. Han, M. K. Tey, and L. You, Deterministic entanglement generation from driving through quantum phase transitions, Science **355**, 620 (2017).
[21] B. C. Sanders, Quantum dynamics of the nonlinear rotator and the effects of continual spin measurement, Phys. Rev. A **40**, 2417 (1989).
[22] A. N. Boto, P. Kok, D. S. Abrams, S. L. Braunstein, C. P. Williams, and J. P. Dowling, Quantum interferometric optical lithography: Exploiting entanglement to beat the diffraction limit, Phys. Rev. Lett. **85**, 2733 (2000).

[23] M. W. Mitchell, J. S. Lundeen, and A. M. Steinberg, Super-resolving phase measurements with a multiphoton entangled state, Nature (London) **429**, 161 (2004).

[24] T. Nagata, R. Okamoto, J. L. O'Brien, K. Sasaki, and S. Takeuchi, Beating the standard quantum limit with four-entangled photons, Science **316**, 726 (2007).

[25] K. Vogel, V. M. Akulin, and W. P. Schleich, Quantum state engineering of the radiation field, Phys. Rev. Lett. **71**, 1816 (1993).

[26] J. Park, Y. Lu, J. Lee, Y. Shen, K. Zhang, S. Zhang, M. S. Zubairy, K. Kim, and H. Nha, Revealing nonclassicality beyond Gaussian states via a single marginal distribution, Proc. Natl. Acad. Sci. USA **114**, 891 (2017).

[27] C. J. Villas-Boas and D. Z. Rossatto, Multiphoton Jaynes-Cummings model: Arbitrary rotations in Fock space and quantum filters, Phys. Rev. Lett. **122**, 123604 (2019).

[28] J. H. Shapiro, S. R. Shepard, and N. C. Wong, Ultimate quantum limits on phase measurement, Phys. Rev. Lett. **62**, 2377 (1989).

[29] J. H. Shapiro and S. R. Shepard, Quantum phase measurement: A system-theory perspective, Phys. Rev. A **43**, 3795 (1991).

[30] S. L. Braunstein, Some limits to precision phase measurement, Phys. Rev. A **49**, 69 (1994).

[31] A. Kowalewska-Kudłaszyk and W. Leoński, Finite-dimensional states and entanglement generation for a nonlinear coupler, Phys. Rev. A **73**, 042318 (2006).

[32] M. G. Genoni, M. G. A. Paris, and K. Banaszek, Measure of the non-Gaussian character of a quantum state, Phys. Rev. A **76**, 042327 (2007).

[33] C. Lee, C. Oh, H. Jeong, C. Rockstuhl, and S.-Y. Lee, Using states with a large photon number variance to increase quantum Fisher information in single-mode phase estimation, J. Phys. Commun. **3**, 115008 (2019).

[34] J.-F. Qin, Y. Xu, and J. Liu, Optimal finite-dimensional probe states for quantum phase estimation, Phys. Rev. A **112**, 052428 (2025).

[35] W. Lu, L. Shao, X. Zhang, Z. Zhang, J. Chen, H. Tao, and X. Wang, Extreme expected values and their applications in quantum metrology, Phys. Rev. A **105**, 023718 (2022).

[36] S.-Y. Lee, C.-W. Lee, J. Lee, and H. Nha, Quantum phase estimation using path-symmetric entangled states, Sci. Rep. **6**, 30306 (2016).

[37] C. C. Gerry, A. Benmoussa, and R. A. Campos, Parity measurements, Heisenberg-limited phase estimation, and beyond, J. Mod. Opt. **54**, 2177 (2007).

[38] C. C. Gerry and J. Mimih, The parity operator in quantum optical metrology, Contemp. Phys. **51**, 497 (2010).

[39] C. C. Gerry and J. Mimih, Heisenberg-limited interferometry with pair coherent states and parity measurements, Phys. Rev. A **82**, 013831 (2010).

[40] W. N. Plick, P. M. Anisimov, J. P. Dowling, H. Lee, and G. S. Agarwal, Parity detection in quantum optical metrology without number-resolving detectors, New J. Phys. **12**, 113025 (2010).

[41] L. Cohen, D. Istrati, L. Dovrat, and H. S. Eisenberg, Super-resolved phase measurements at the shot noise limit by parity measurement, Opt. Express **22**, 11945 (2014).

[42] K. Banaszek and I. A. Walmsley, Photon counting with a loop detector, Opt. Lett. **28**, 52 (2003).

[43] M. J. Fitch, B. C. Jacobs, T. B. Pittman, and J. D. Franson, Photon-number resolution using time-multiplexed single-photon detectors, Phys. Rev. A **68**, 043814 (2003).

[44] C. Silberhorn, Detecting quantum light, Contemp. Phys. **48**, 143 (2007).

[45] H.-S. Zhong, Y. Li, W. Li, L.-C. Peng, Z.-E. Su, Y. Hu, Y.-M. He, X. Ding, W. Zhang, H. Li, L. Zhang, Z. Wang, L. You, X.-L. Wang, X. Jiang, L. Li, Y.-A. Chen, N.-L. Liu, C.-Y. Lu, and J.-W. Pan, 12-photon entanglement and scalable scattershot boson sampling with optimal entangled-photon pairs from parametric down-conversion, Phys. Rev. Lett. **121**, 250505 (2018).

[46] J. Tiedau, M. Engelkemeier, B. Brecht, J. Sperling, and C. Silberhorn, Statistical benchmarking of scalable photonic quantum systems, Phys. Rev. Lett. **126**, 023601 (2021).

[47] D. W. Berry and H. M. Wiseman, Optimal states and almost optimal adaptive measurements for quantum interferometry, Phys. Rev. Lett. **85**, 5098 (2000).

[48] D. W. Berry, H. M. Wiseman, and J. K. Breslin, Optimal input states and feedback for interferometric phase estimation, Phys. Rev. A **63**, 053804 (2001).

[49] I. Bargatin, Mutual information-based approach to adaptive homodyne detection of quantum optical states, Phys. Rev. A **72**, 022316 (2005).

[50] R. Demkowicz-Dobrzański, J. Czajkowski, and P. Sekatski, Adaptive quantum metrology under general Markovian noise, Phys. Rev. X **7**, 041009 (2017).

[51] M. A. Rodríguez-García, M. T. DiMario, P. Barberis-Blostein, and F. E. Becerra, Determination of the asymptotic limits of adaptive photon counting measurements for coherent-state optical phase estimation, npj Quantum Inf. **8**, 94 (2022).

[52] S. Kurdziałek, W. Górecki, F. Albarelli, and R. Demkowicz-Dobrzański, Using adaptiveness and causal superpositions against noise in quantum metrology, Phys. Rev. Lett. **131**, 090801 (2023).

[53] F. Albarelli and R. Demkowicz-Dobrzański, Probe incompatibility in multiparameter noisy quantum metrology, Phys. Rev. X **12**, 011039 (2022).

[54] S. Sieniawski and R. Demkowicz-Dobrzański, Adaptive quantum channel discrimination using methods of quantum metrology, New J. Phys. **28**, 024502 (2026).

[55] J. Liu, M. Zhang, H. Chen, L. Wang, and H. Yuan, Optimal scheme for quantum metrology, Adv. Quantum Technol. **5**, 2100080 (2022).

[56] M. A. Taylor, J. Janousek, V. Daria, J. Knittel, B. Hage, H.-A. Bachor, and W. P. Bowen, Biological measurement beyond the quantum limit, Nat. Photon. **7**, 229 (2013).

[57] C.-Y. Lu, Y. Cao, C.-Z. Peng, and J.-W. Pan, Micius quantum experiments in space, Rev. Mod. Phys. **94**, 035001 (2022).

[58] H. S. Stokowski, T. P. McKenna, T. Park, A. Y. Hwang, D. J. Dean, O. T. Celik, V. Ansari, M. M. Fejer, and A. H. Safavi-Naeini, Integrated quantum optical phase sensor in thin film lithium niobate, Nat. Commun. **14**, 3355 (2023).

[59] S. D. Huver, C. F. Wildfeuer, and J. P. Dowling, Entangled Fock states for robust quantum optical metrology, imaging, and sensing, Phys. Rev. A **78**, 063828 (2008).

[60] R. Demkowicz-Dobrzański, U. Dorner, B. J. Smith, J. S. Lundeen, W. Wasilewski, K. Banaszek, and I. A. Walmsley, Quantum phase estimation with lossy interferometers, Phys. Rev. A **80**, 013825 (2009).

[61] U. Dorner, R. Demkowicz-Dobrzański, B. J. Smith, J. S. Lundeen, W. Wasilewski, K. Banaszek, and I. A. Walmsley, Optimal quantum phase estimation, Phys. Rev. Lett. **102**, 040403 (2009).

[62] T.-W. Lee, S. D. Huver, H. Lee, L. Kaplan, S. B. McCracken, C. Min, D. B. Uskov, C. F. Wildfeuer, G. Veronis, and J. P. Dowling, Optimization of quantum interferometric metrological sensors in the presence of photon loss, Phys. Rev. A **80**, 063803 (2009).

[63] K. Jiang, C. J. Brignac, Y. Weng, M. B. Kim, H. Lee, and J. P. Dowling, Strategies for choosing path-entangled number states for optimal robust quantum-optical metrology in the presence of loss, Phys. Rev. A **86**, 013826 (2012).

[64] J. Liu, X. Jing, and X. Wang, Phase-matching condition for enhancement of phase sensitivity in quantum metrology, Phys. Rev. A **88**, 042316 (2013).

[65] P. A. Knott, T. J. Proctor, Kae Nemoto, J. A. Dunningham, and W. J. Munro, Effect of multimode entanglement on lossy optical quantum metrology, Phys. Rev. A **90**, 033846 (2014).

[66] P. A. Knott, T. J. Proctor, A. J. Hayes, J. P. Cooling, and J. A. Dunningham, Practical quantum metrology with large precision gains in the low-photon-number regime, Phys. Rev. A **93**, 033859 (2016).

[67] S.-Y. Lee, Y. S. Ihn, and Z. Kim, Optimal entangled coherent states in lossy quantum-enhanced metrology, Phys. Rev. A **101**, 012332 (2020).

[68] M. J. D. Powell, *Advances in Optimization and Numerical Analysis* (Springer, New York, 1994).

[69] M. J. D. Powell, Direct search algorithms for optimization calculations, Acta Numer. **7**, 287 (1998).

[70] M. J. D. Powell, A view of algorithms for optimization without derivatives, Math. TodayBull. Inst. Math. Appl. **43**, 170 (2007).

[71] C. W. Helstrom, *Quantum Detection and Estimation Theory* (Academic Press, New York, 1976).

[72] A. S. Holevo, *Probabilistic and Statistical Aspects of Quantum Theory* (North-Holland, Amsterdam, 1982).

[73] J. Liu, X.-X. Jing, and X. Wang, Quantum metrology with unitary parametrization processes, Sci. Rep. **5**, 8565 (2015).

[74] J. Liu, H. Yuan, X-M. Lu, and X. Wang, Quantum Fisher information matrix and multiparameter estimation, J. Phys. A: Math. Theor. **53**, 023001 (2020).

[75] J. Liu, X.-X. Jing, W. Zhong, and X. Wang, Quantum Fisher information for density matrices with arbitrary ranks, Commun. Theor. Phys. **61**, 45 (2014).

[76] M. Zhang, H.-M. Yu, H. Yuan, X. Wang, R. Demkowicz-Dobrzański, and J. Liu, QuanEstimation: An open-source toolkit for quantum parameter estimation, Phys. Rev. Res. **4**, 043057 (2022).

[77] H.-M. Yu and J. Liu, Quanestimation.jl: An open-source Julia framework for quantum parameter estimation, Fundam. Res. (2025).

[78] H. M. Wiseman and R. B. Killip, Adaptive single-shot phase measurements: A semiclassical approach, Phys. Rev. A **56**, 944 (1997).

[79] G. Frascella, S. Agne, F. Ya Khalili, and M. V. Chekhova, Overcoming detection loss and noise in squeezing-based optical sensing, npj Quantum Inf. **7**, 72 (2021).

[80] J.-F. Qin and J. Liu, Optimal noisy quantum phase estimation with finite-dimensional states, Zenodo (2026), doi:10.5281/zenodo.16788840.